

RESEARCH ARTICLE

# LittleBrain: A gradient-based tool for the topographical interpretation of cerebellar neuroimaging findings

Xavier Guell<sup>1,2\*</sup>, Mathias Goncalves<sup>1</sup>, Jakub R. Kaczmarzyk<sup>1</sup>, John D. E. Gabrieli<sup>1</sup>, Jeremy D. Schmahmann<sup>2,3</sup>, Satrajit S. Ghosh<sup>1,4</sup>

**1** McGovern Institute for Brain Research, Massachusetts Institute of Technology, Cambridge, Massachusetts, United States of America, **2** Laboratory for Neuroanatomy and Cerebellar Neurobiology, Department of Neurology, Massachusetts General Hospital, Harvard Medical School, Boston, Massachusetts, United States of America, **3** Ataxia Unit, Cognitive Behavioral Neurology Unit, Department of Neurology, Massachusetts General Hospital, Harvard Medical School, Boston, Massachusetts, United States of America, **4** Department of Otolaryngology, Harvard Medical School, Boston, Massachusetts, United States of America

\* [xaviergp@mit.edu](mailto:xaviergp@mit.edu)



**OPEN ACCESS**

**Citation:** Guell X, Goncalves M, Kaczmarzyk JR, Gabrieli JDE, Schmahmann JD, Ghosh SS (2019) LittleBrain: A gradient-based tool for the topographical interpretation of cerebellar neuroimaging findings. *PLoS ONE* 14(1): e0210028. <https://doi.org/10.1371/journal.pone.0210028>

**Editor:** Daniel S. Margulies, Max Planck Institute for Human Cognitive and Brain Sciences, GERMANY

**Received:** September 17, 2018

**Accepted:** December 14, 2018

**Published:** January 16, 2019

**Copyright:** © 2019 Guell et al. This is an open access article distributed under the terms of the [Creative Commons Attribution License](https://creativecommons.org/licenses/by/4.0/), which permits unrestricted use, distribution, and reproduction in any medium, provided the original author and source are credited.

**Data Availability Statement:** All code and data can be found in our github repository (<https://github.com/xaviergp/littlebrain>), docker hub container (<https://hub.docker.com/r/xaviergp/littlebrain>), and neurovault (<https://neurovault.org/collections/2531>), as specified in the manuscript.

**Funding:** This study was supported by La Caixa Banking Foundation (XG), the MGH ECOR Fund for Medical Discovery Postdoctoral Fellowship Award

## Abstract

Gradient-based approaches to brain function have recently unmasked fundamental properties of brain organization. Diffusion map embedding analysis of resting-state fMRI data revealed a primary-to-transmodal axis of cerebral cortical macroscale functional organization. The same method was recently used to analyze resting-state data within the cerebellum, revealing for the first time a sensorimotor-fugal macroscale organization principle of cerebellar function. Cerebellar gradient 1 extended from motor to non-motor task-unfocused (default-mode network) areas, and cerebellar gradient 2 isolated task-focused processing regions. Here we present a freely available and easily accessible tool that applies this new knowledge to the topographical interpretation of cerebellar neuroimaging findings. LittleBrain illustrates the relationship between cerebellar data (e.g., volumetric patient study clusters, task activation maps, etc.) and cerebellar gradients 1 and 2. Specifically, LittleBrain plots all voxels of the cerebellum in a two-dimensional scatterplot, with each axis corresponding to one of the two principal functional gradients of the cerebellum, and indicates the position of cerebellar neuroimaging data within these two dimensions. This novel method of data mapping provides alternative, gradual visualizations that complement discrete parcelation maps of cerebellar functional neuroanatomy. We present application examples to show that LittleBrain can also capture subtle, progressive aspects of cerebellar functional neuroanatomy that would be difficult to visualize using conventional mapping techniques. Download and use instructions can be found at <https://xaviergp.github.io/littlebrain>.

## Introduction

Neuroimaging research has greatly improved our knowledge of brain function and structure in health and disease. It has revealed that specific brain regions are associated with specific

(XG), the MINDLink foundation (JDS), and National Institutes of Health R01 EB020740 (SSG) and P41 EB019936 (SSG). The funders had no role in study design, data collection and analysis, decision to publish, or preparation of the manuscript. There was no additional external funding received for this study.

**Competing interests:** The authors have declared that no competing interests exist.

neurological functions, a territory of knowledge that was previously accessible only through the study of patients with brain injury. It has also provided the first compelling evidence that neuropsychiatric and neurodevelopmental disorders are associated with disruptions in brain structure and function, described brain organization features that can change from subject to subject, and provided new measures that may predict future human behavior such as treatment response in neurology and psychiatry [1].

Topographic interpretation of neuroimaging findings is crucial to the neuroimaging field's mission to understand the nervous system and alleviate suffering in neurological and psychiatric disorders. Studies often reveal brain activation related to a specific aspect of cognitive processing or brain structural changes associated with a neurological disorder. These findings immediately lead to a topographical interpretation question—what does the distribution of these findings mean? One approach to answer this question is to delineate brain regions and interpret the distribution of these findings based on their overlap with these regions. For example, one may parcellate the cerebral cortex into seven distinct networks (somatomotor, visual, ventral and dorsal attention, frontoparietal, limbic, and default-mode network; calculated using a clustering algorithm that analyzes similarity of resting-state functional connectivity between all data points in the cerebral cortex) [2]. The topographical distribution of a cerebral cortical neuroimaging cluster may then be interpreted based on its overlap with these seven regions. Here we propose a different approach to the topographical interpretation of neuroimaging findings based on the utilization of continuous (“gradients”) rather than discrete functionally-defined brain maps.

Several recent studies have adopted gradient-based approaches to describe brain organization. Margulies and colleagues [3] used diffusion map embedding [4] to extract functional gradients from fMRI resting-state data and described two gradients that offer a continuous measure of cerebral cortical functional organization. Gradient 1 extended from primary cortices to transmodal association areas (default-mode network), and gradient 2 extended from primary visual to primary motor/somatosensory and auditory cortical areas [3]. A recent review [5] related these findings to other gradient-based analyses of cerebral cortical T1 intensity (a proxy measure of myelin content) [6], neuroimaging measures of semantic representation [7], and neuroimaging measures of variations in the timescale of event representation [8]. These findings are contextualized within a larger research program where noninvasive imaging measures of connectivity guide the characterization of functional organization in the human brain [9,10], and a large body of pre-existing literature that used gradient-based approaches to characterize functional or structural connectivity in primary motor cortex [11], primary visual cortex [11], entorhinal cortex [12], insula [13], temporal lobe [14,15], and striatum [16]. Diffusion map embedding was recently used to analyze resting-state data within the cerebellum, revealing for the first time a sensorimotor-fugal macroscale organization of cerebellar function [17]. Cerebellar gradient 1 extended from motor to non-motor task-unfocused (default-mode) areas, and cerebellar gradient 2 progressed from task-focused to task-unfocused processing regions [17]. Gradient-based approaches to brain organization have thus provided novel insights into the functional organization of the brain.

Here we explore the application of this new knowledge to the topographical interpretation of cerebellar neuroimaging findings. Specifically, we aimed to develop a user-friendly tool that ought to facilitate the adoption of a novel gradient-based cerebellar data visualization approach in the neuroimaging community. To achieve this, we minimized installation requirements, maximized user-friendly features, and also empowered experienced users to visualize and modify any features of our tool.

The cerebellum has recently become scientifically relevant not only for the study of motor processes, but also for the study of all complex neurological functions. A large body of

literature has shown that the cerebellum is anatomically connected to motor as well as non-motor aspects of the extra-cerebellar structures, that the cerebellum is engaged in numerous motor as well as non-motor aspects of task activation and functional connectivity measures in neuroimaging studies, and that isolated cerebellar injury generates not only a cerebellar motor syndrome but also a cerebellar cognitive affective syndrome [18,19,28–37,20,38,21–27]. Similarly, the cerebellum has become clinically relevant for the study of not only primary cases of cerebellar injury or degeneration, but also neurology and psychiatry as a whole. Numerous studies have revealed that many neurological and psychiatric diseases that impair cognitive and affective processing include cerebellar functional and structural abnormalities [39–47]. In this way, the present article describes the development of a novel, timely, and relevant neuroscience tool.

## Methods

### Methods overview

LittleBrain illustrates the relationship between cerebellar data (e.g., volumetric patient study clusters, task activation maps, etc.) and cerebellar gradients 1 and 2. Specifically, LittleBrain plots all voxels of the cerebellum in a two-dimensional scatterplot, with each axis corresponding to one of the two principal functional gradients of the cerebellum, and indicates the position of cerebellar neuroimaging data within these two dimensions. A manual with detailed download and use instructions is available at <https://xaviergp.github.io/littlebrain> [48]. The user of our tool will download and install Docker (<https://docker.com>). With Docker, the user will download a container that includes a fixed set of all the files and software dependencies required to use our tool. The user will provide, as input, a neuroimaging file that contains cerebellar data. Our tool will then generate a plot that illustrates the relationship between the spatial distribution of these data and the two principal functional gradients of the cerebellum. These two gradients were developed in a previous study by Guell and colleagues [17] using diffusion map embedding [4] (see <https://github.com/satra/mapalign> for an implementation). Diffusion map embedding is a dimensionality reduction technique that can be used to analyze the similarity between connectivity patterns of all data points within a given brain structure. Connectivity from each data point to all (n) data points is represented as an n-dimensional vector. Similarity of connectivity between each pair of data points is calculated based on cosine distance between each pair of vectors. This measure of similarity is then used to represent the probability of transition between each pair of data points in a Markov chain. This probability of transition can be analyzed as a symmetric transformation matrix, thereby enabling the calculation of eigenvectors. These eigenvectors represent the principle orthogonal directions of transitions between all pairs of data points—or “functional gradients”. This approach is similar to that described by Haak and colleagues (“connectopies”) [11], with minor differences in the specific methods used to calculate similarity matrices, Laplacians, and scaling of eigenspectra. Haak and colleagues developed a toolbox (“Congrads”; <https://github.com/koenhaak/congrads>) which in contrast to LittleBrain is used to calculate functional gradients (or “connectopies”), rather than to visualize cerebellar neuroimaging data in relationship to pre-defined functional gradients of the cerebellum. In the cerebellum, Gradient 1 represents a gradual transition from motor to task-unfocused cognitive processing. Gradient 2 isolates task-focused cognitive processing (Fig 1 illustrates the functional interpretation of cerebellar functional gradients 1 and 2, based on their relationship with task activation maps and previous resting-state parcellations of the cerebellum). Cerebellar voxels that are close in gradient 1 and gradient 2 dimensions have similar functional connectivity patterns. Cerebellar voxels that are distant in gradient 1 dimension have distinct functional connectivity patterns, specifically

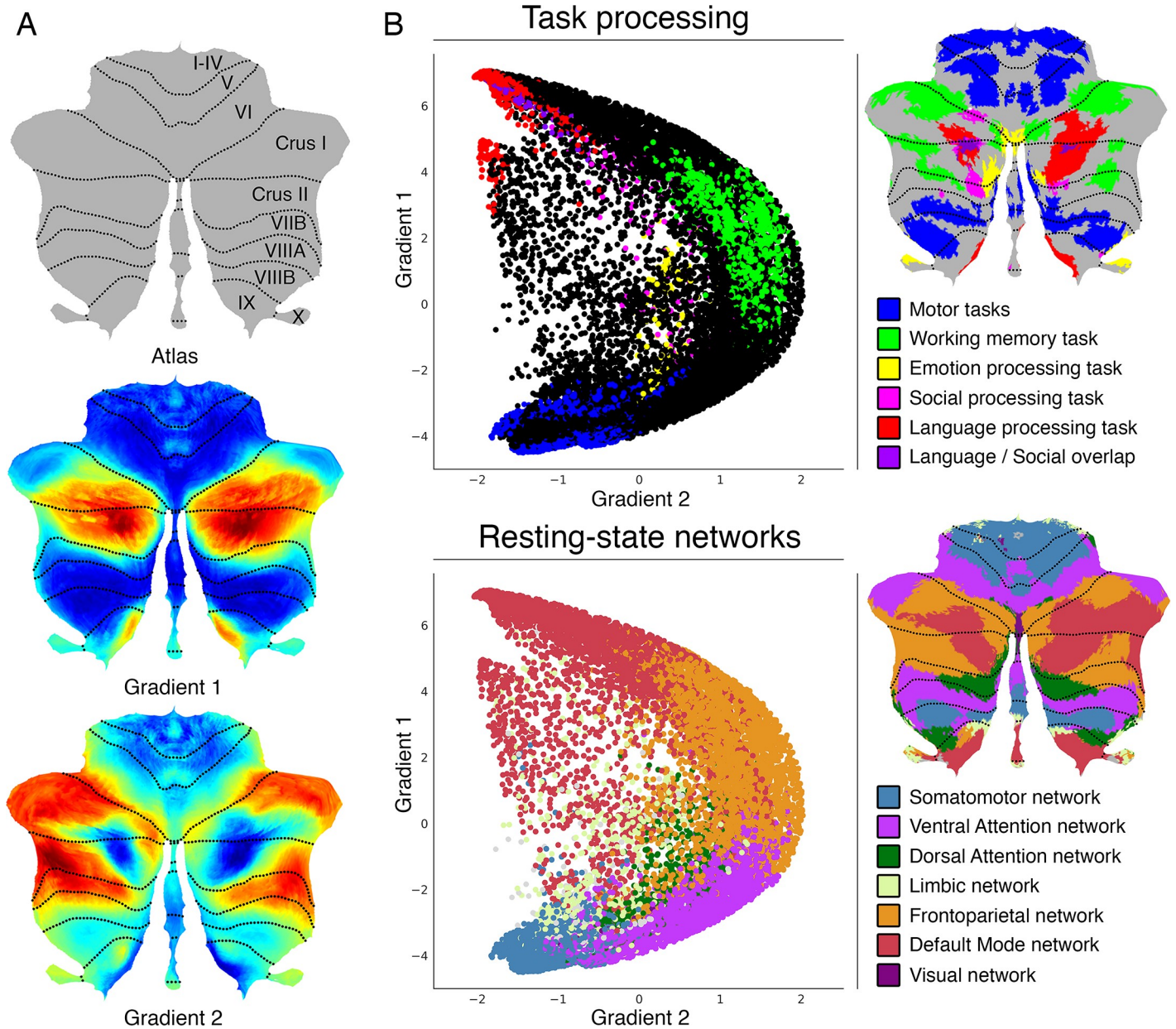


**Fig 1. Cerebellum functional gradients and their relationship with discrete task activation and resting-state maps.** Adapted with permission from Guell et al., 2018 [17]. Gradient 1 extends from motor to task-unfocused cognitive processing regions. Specifically, gradient 1 extends from language task (story listening minus math task contrast, isolating task-unfocused cognitive processing) / Default Mode Network regions to motor regions. Gradient 2 isolates task-focused cognitive processing. Specifically, gradient 2 isolates working memory task processing / task-positive cognitive network areas. (A) Gradients 1 and 2 are shown in a color scale from blue to red. (B) A scatterplot of gradient 1 and 2 illustrating their relationship with task (from Guell et al., 2018 [49]) and resting-state maps (from Buckner et al., 2011 [50]). Each dot corresponds to a cerebellar voxel, position of each dot along x and y axis corresponds to position along Gradient 1 and Gradient 2 for that cerebellar voxel, and color of the dot corresponds to task activation (top) or resting-state network (bottom) associated with that particular voxel.

<https://doi.org/10.1371/journal.pone.0210028.g001>

as determined by their relationship to the connectivity patterns of motor as opposed to task-unfocused cognitive processing areas of the cerebellum. Restated, gradient 1 captures a progression from those aspects of the cerebellum that are engaged in motor control to those aspects of the cerebellum that are engaged in task-unfocused cognitive processing (mind wandering, goal-undirected thought). Cerebellar voxels that are distant in gradient 2 dimension

have distinct functional connectivity patterns, specifically as determined by their relationship to the connectivity patterns of task-focused cognitive processing areas as opposed to the rest of the areas of the cerebellum. Restated, gradient 2 isolates those aspects of the cerebellum that are engaged in task-focused cognitive processing (attentive, goal-directed thought).

## Input

Neuroimaging data provided by the user must be registered to MNI152 space and be in NIfTI (.nii or .nii.gz) format. This NIfTI file may include clusters outside of the cerebellum, and clusters within the cerebellum may extend outside the cerebellum or inside cerebellar white matter—these portions of the data will be removed as part of our preprocessing algorithm. The input may correspond to volumetric patient study clusters, task activation maps, or any form of cerebellar three-dimensional data that the user might wish to visualize in relationship to cerebellar functional gradients. Further, the input does not need to be thresholded or binarized—the user will have the option to select a threshold value when selecting the input, and thresholding and binarization will be performed automatically. For example, if the input data correspond to Z statistics of an fMRI task activation contrast, the user might choose to only visualize data above a specific value of the Z statistics.

## Data preprocessing

Preprocessing steps include (i) binarization (and thresholding and/or no binarization if selected by the user) using FSL's `fslmaths` [51], (ii) downsampling to 2mm resolution using FSL's FLIRT (FMRIB'S Linear Image Registration Tool) [51–53], (iii) adding or deleting slices to match the Human Connectome's mask files using FSL's `fslroi` [51], (iv) masking according to the cerebellum gray matter mask from the Human Connectome Project using Freesurfer's `mrmask` [54], so that extra-cerebellar structures as well as white matter aspects of the cerebellum are removed, (v) transforming image size characteristics of the image to match the Human Connectome Project image size characteristics using FSL's FLIRT [51–53], and (vi) reformatting the image from NIfTI to CIFTI dscalar format using Workbench Command's `-cifti-create-dense-from-template` [55].

## Gradients map formation

Following pre-processing, Python-based calculations generate arrays corresponding to gradient 1 and gradient 2 values (as provided by Guell et al., 2018 [17]) for each cerebellar voxel, as well as an equally-sized array consisting of either 1 or 0 values for each cerebellar voxel equivalent to the thresholded and binarized cerebellar data provided by the user. A two-dimensional scatterplot is then generated using `matplotlib` and `seaborn`, where each dot in the scatterplot represents a cerebellar voxel, position of each dot along x and y axis corresponds to position along gradient 1 and gradient 2 for that cerebellar voxel, and dots shown in red correspond to the voxels that are included in the cerebellar cluster provided by the user. The user will also have the option to visualize (i) a non-binary version of gradient maps, where color intensity corresponds to the values in the data that were entered as input, and (ii) a network-colored version of gradient maps, where color corresponds to the resting-state network associated with each voxel (based on Buckner et al., 2011 [50]). Comma-separated values (CSV) files containing a list of gradient 1 and gradient 2 values for the cerebellar data entered as input are automatically saved. Before re-starting the process to generate a new map, intermediate files are automatically removed.

## Quality control

While we were unable to identify cases where an MNI-registered NIfTI file was incorrectly transformed, it remains a possibility that preprocessing steps described in this section might result in an erroneous position of the transformed cluster. Extra-cerebellar and cerebellar white matter portions of the data should be removed, but portions of the cluster in cerebellar grey matter should not change their location after preprocessing. The user will have the option to visualize two glass-brain images automatically generated using niwidget to make sure that no erroneous transformations have occurred. Restated, the user will have the option to visualize that position of cerebellar grey matter data has not changed as a result of preprocessing.

## Docker container: Simplicity and reproducibility

The processing steps described here require multiple software packages (FSL [51], Freesurfer [54], Connectome Workbench [55], Python 3, and multiple Python packages). The requirement to install these programs would decrease the accessibility of our tool. Further, software updates in these programs might disrupt correct functioning of our tool in the future, or generate replication failures across laboratories. To address these issues, we packaged our tool and all its files and software dependencies in a “Docker container” [56] using neurodocker [57]. Docker [56] is an open source project that allows the encapsulation of multiple software packages and files into a single “container”. This container can be stored online in a public repository, be easily downloaded by users worldwide, and guarantees that any computer will be able to perform all operations inside the container in the same way. Users will need to install Docker on their computers, and will be able to use our tool by simply downloading and running one single Docker container. No software paid subscriptions are required to use our tool. However, if you are considering commercial use of FSL, please consult their license at <https://fsl.fmrib.ox.ac.uk/fsl/fslwiki/Licence>. Our Docker container has been minimized using reprozip [58], and hence includes only those aspects of FSL, Freesurfer, and Connectome Workbench that are necessary to perform the functions of LittleBrain. This reduced the size of LittleBrain to 2.5 gigabytes (compared to 12 gigabytes if we had not performed this minimizing step).

## Jupyter Notebook: Transparency and flexibility

LittleBrain is run interactively using Jupyter Notebook [59]. Jupyter Notebook is a browser application that allows users to code interactively, display graphics, and enter user input. In this way, while our tool displays figures (gradient 1/2 scatterplot, quality control output), accepts user input using text boxes, and provides an intuitive interface, it also exposes the code for each step of the process, and allows users with coding experience to visualize and modify any feature of our tool. Examples of the flexibility that Jupyter Notebook provides are given in the following section.

## Ethics statement

Cerebellar functional gradients were obtained from a previous study by Guell and colleagues [17]; for data used to generate these gradients, written consent forms were previously approved by the Washington University Institutional Review Board as part of the Human Connectome Project, which was performed according to the principles expressed in the Declaration of Helsinki.

For Application example 1 (see below), all participants provided written, informed consent in accordance with the Massachusetts Institute of Technology Institutional Review Board (full

name: "Massachusetts Institute of Technology Committee on the Use of Humans as Experimental Subjects" (COUHES)), and the study was performed according to the principles expressed in the Declaration of Helsinki. The Massachusetts Institute of Technology Committee on the Use of Humans as Experimental Subjects specifically reviewed and approved this study.

For Application example 2 (see below), data was obtained from Neurovault from a previous study by Lesage and colleagues [60]; for this study all participants provided written informed consent, the study was approved by the local ethics committee at the University of Birmingham, and was performed according to the principles expressed in the Declaration of Helsinki.

## Results

In this section we describe the architecture and features of LittleBrain (Fig 2) and present two example analyses. Three additional examples are then shown to illustrate alternative visualization strategies that experienced users might implement by using the interactive Jupyter notebook.

### Application example 1

An unpublished study from our laboratory used multi-voxel pattern analysis (MVPA) to identify brain regions with abnormal whole-brain functional connectivity patterns in a patient with a retrocerebellar arachnoid cyst compressing the cerebellum and a life-long history of psychiatric and neurodevelopmental symptoms. The patient's data was compared to 36 healthy controls. This analysis revealed a cluster in cerebellar lobules I through VI (Fig 3(A)). Lobules I-VI are engaged in motor processing. Multiple studies also indicate a non-motor role of some aspects of lobule VI [29,32,33,49]. A cerebellar resting-state network map [50] revealed overlap with somatosensory network as well as some aspects of ventral attention network (Fig 3(B)), indicating that this cluster may include predominantly motor (somatomotor network) but also non-motor task-focused cognitive processing regions (ventral attention network). LittleBrain provided an alternative, clear visualization of this concept (Fig 3(C)). Most voxels of the cerebellar cluster had low gradient 1 / low gradient 2 values, indicating a strong inclusion of motor processing regions. As expected, a few voxels extended towards task-focused cognitive processing regions (i.e. high gradient 2 values). LittleBrain can thus provide alternative, gradual visualizations that complement discrete parcellation maps of cerebellar functional neuroanatomy. This example can be reproduced by mapping the "example.nii" file included in LittleBrain.

### Application example 2

A study by Lesage and colleagues [60] performed two localizer task experiments in a group of 18 healthy participants. The "Semantic" working memory task contrasted a 1-back condition (while watching pictures of objects, press a button if the semantic category of the present image is the same as the semantic category of the previous image; e.g., press the button if the picture of a sailing boat is followed by a picture of a motor boat, but not if a picture of a sailing boat is followed by a picture of a fish) minus a 0-back condition (similar pictures are shown, and participants are required to press the button when a target image appears, e.g. press the button every time the picture of a sailing boat appears in the screen). Of note, subjects were previously familiarized with 10 stimulus categories: cycles, birds, boats, dogs, fish, fruits, buildings, shoes, tools, and furniture. The "Punjabi" working memory task contrasted a 1-back condition (while watching pictures of incomprehensible Punjabi alphabet pseudowords, press a button if the pseudoword of the present image is the same as the pseudoword of the previous image) minus a 0-back condition (similar pictures are shown, and participants are required to

```
example.nii
example_2.nii
example_3.nii
example_4.nii
```

The list above shows the nifti files you have uploaded in the "LOAD\_NIFTI\_FILE\_HERE" folder. Note that these nifti files must be in MNI space. Copy name of nifti file you want to map (including the ".nii" termination) and paste it in the box below:

Write a threshold number in the box below if you want to threshold your file; if no threshold leave blank:

Generate map

Generating map for: example.nii  
Threshold selected: 0.1  
Please wait...

Map generated for: example.nii  
Threshold selected: 0.1  
To save the map go to the "OUTPUT\_FILES" folder in the other opened tab in your browser, and download "MAP.png". You can also right click the image below and select "save image as". What do you want to do next?:

Check transformations

See non-binary map

See network-colored map

Generate a new map

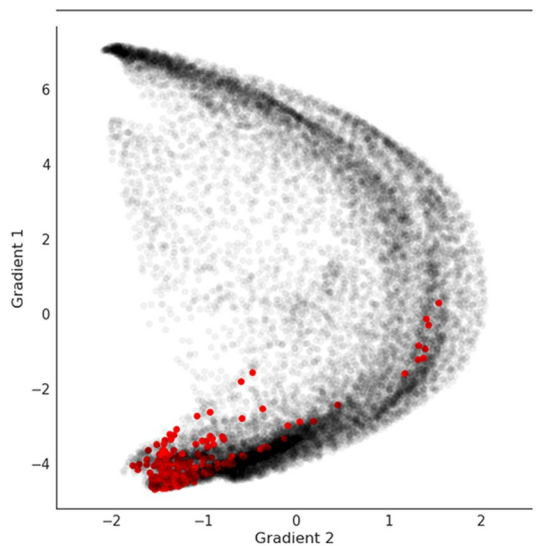


IMAGE 1. Each black dot in the scatterplot represents a cerebellar voxel, position of each dot along x and y axis corresponds to position along gradient 1 and gradient 2 for that cerebellar voxel, and dots shown in red correspond to the voxels that are included in the uploaded file.



IMAGE 1. This is the thresholded cluster you have uploaded.

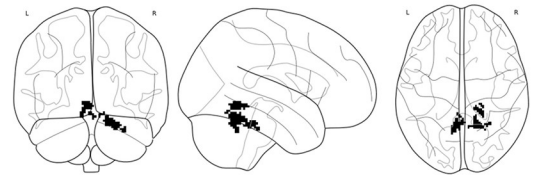
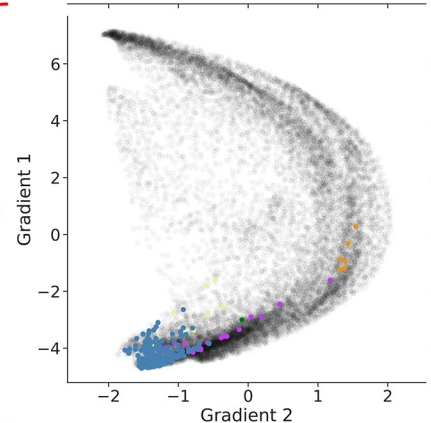
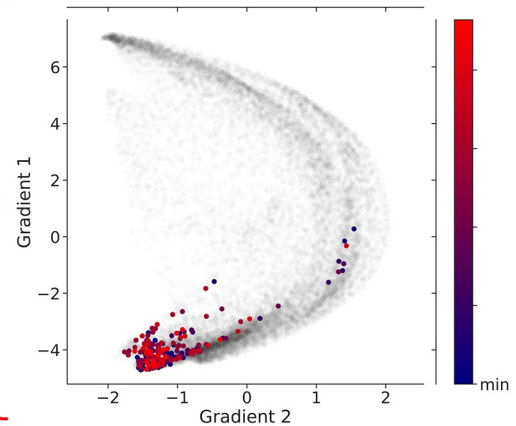


IMAGE 2. This is a cerebellum-masked, 2mm resolution version of the cluster that has been created to generate the map. Note that non-cerebellar parts of the cluster are removed in image 2, as well as parts of the cluster which are in cerebellar white matter. For this reason, the cluster in image 2 might look smaller (indicating that some parts of the cluster you uploaded were outside of the cerebellum, or in cerebellar white matter). To examine this further in your computer, you can access the transformed image by downloading "image\_binarized\_2mm\_resliced\_cerebellummasked\_postsecondFLIRT.nii" from the "OUTPUT\_FILES" folder and comparing it to the initial nifti file you uploaded. If you want to do this, make sure that you download this image before generating a new map, as files will be over-written.



**Fig 2. User interface of LittleBrain.** After uploading NIFTI files containing cerebellar data and running the Jupyter notebook, LittleBrain shows a list of all inputs that have been uploaded. The user enters the name of the input NIFTI file that will be mapped and may also enter a threshold value to be applied to the NIFTI file. After clicking "Generate gradients map" and waiting a few seconds, the screen will display a scatterplot illustrating the relationship of cerebellar data with gradients 1 and 2 from Guell et al., 2018 [17]. In the scatterplot, each dot corresponds to a cerebellar voxel, position of each dot along x and y axis corresponds to position along Gradient 1 and Gradient 2 for that cerebellar voxel, and red dots indicate which cerebellar voxels are included in the data provided by the user after thresholding and binarization. The user will then have the option to quality control by clicking "Check transformations". This option displays two glass-brain images corresponding to



the binarized and thresholded cluster before (top image) and after (bottom image) preprocessing transformations have occurred. Extra-cerebellar and cerebellar white matter portions of the data should be removed, but portions of the cluster in cerebellar grey matter should not change their location after preprocessing. The user will also have the option to visualize (i) a non-binary version of the same map, where color intensity corresponds to the values in the data that were entered as input, and (ii) a network-colored version of the same map, where color corresponds to the resting-state network associated with each voxel (see bottom panel in Fig 1(B); color code as in Buckner et al., 2011 [50]; blue = somatomotor network, purple = ventral attention network, green = dorsal attention network, cream = limbic network, orange = frontoparietal network, red = default mode network, dark purple = visual network). CSV files containing a list of gradient 1 and gradient 2 values for the cerebellar data entered as input are automatically saved in the output folder.

<https://doi.org/10.1371/journal.pone.0210028.g002>

press the button when a target pseudoword appears) (see Fig 4). Task contrast cluster-extent correction based thresholded maps from these analyses were downloaded from Neurovault [61], and we performed additional thresholding (values > 6) to better visualize differences between the two maps.

Both tasks engaged non-motor aspects of the cerebellum [62], specifically lobules VI, Crus I/II, and VIIB (Fig 5). A cerebellar resting-state networks map [50] revealed engagement of ventral/dorsal attention and frontoparietal networks in both tasks, as well as marginal encroachment of default mode network areas in the Semantic task only (Fig 5). Approximation to default mode network regions in the Semantic task might reflect partial engagement of

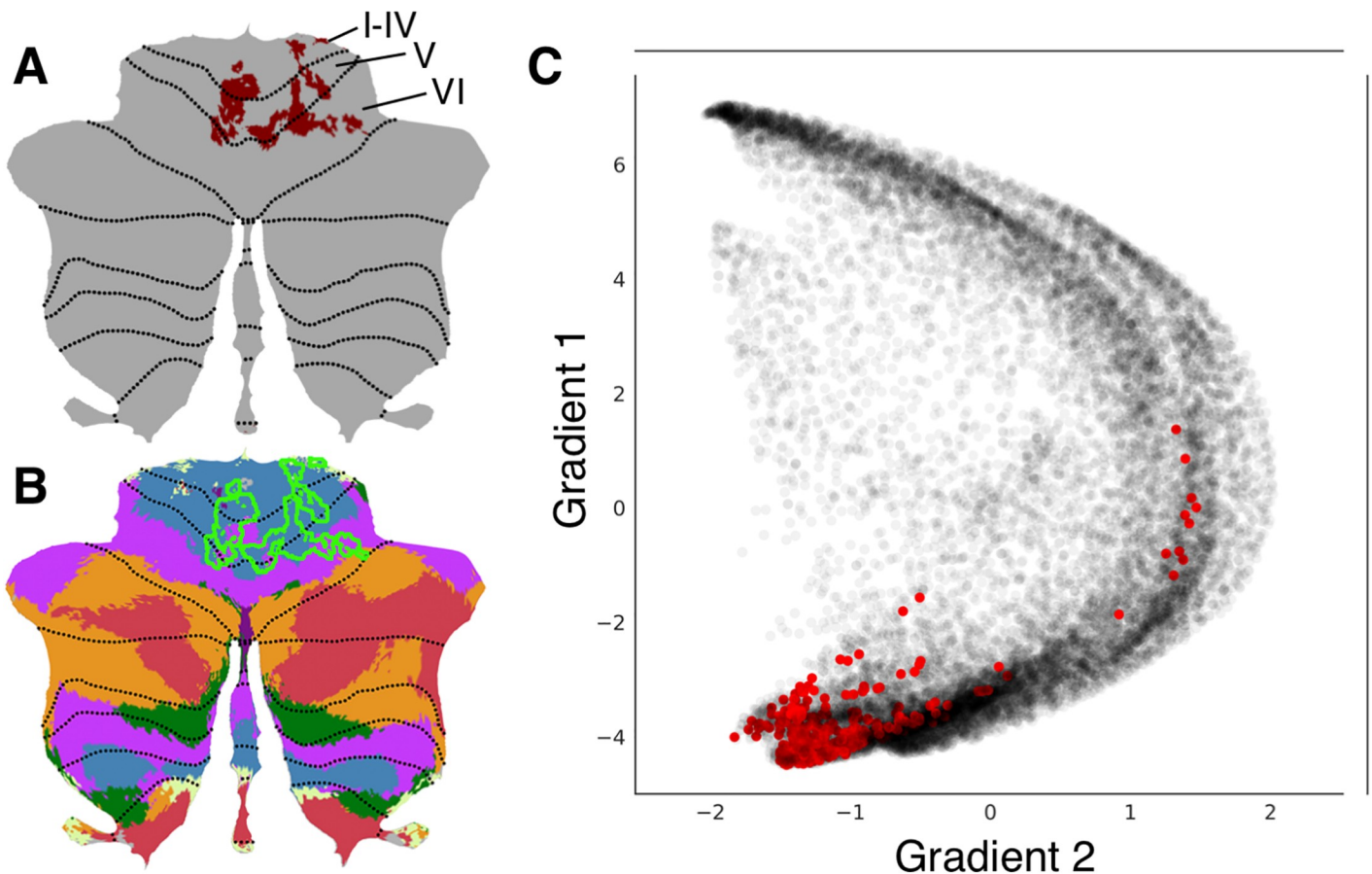


**Fig 3. LittleBrain provides alternative, gradual visualizations that complement discrete parcellation maps of cerebellar functional neuroanatomy.** (A) Cerebellar MVPA cluster (red) was located in lobules I-VI. (B) Overlap of this cluster (green outline) with a resting-state networks map [50] revealed overlap with somatosensory network (blue) as well as some aspects of ventral attention network (purple). (C) Each dot corresponds to a cerebellar voxel, position of each dot along x and y axis corresponds to position along gradients 1 and 2 for that cerebellar voxel, and red dots correspond to those cerebellar voxels that are included in the cerebellar cluster shown in A. This provides an unparalleled, clear visualization of the concept that this cerebellar cluster is mainly localized in motor processing regions (low gradient 1 / low gradient 2 values) but also encroaches task-positive cognitive processing areas (high gradient 2 values).

<https://doi.org/10.1371/journal.pone.0210028.g003>

### SEMANTIC 1-BACK TASK

### PUNJABI 1-BACK TASK

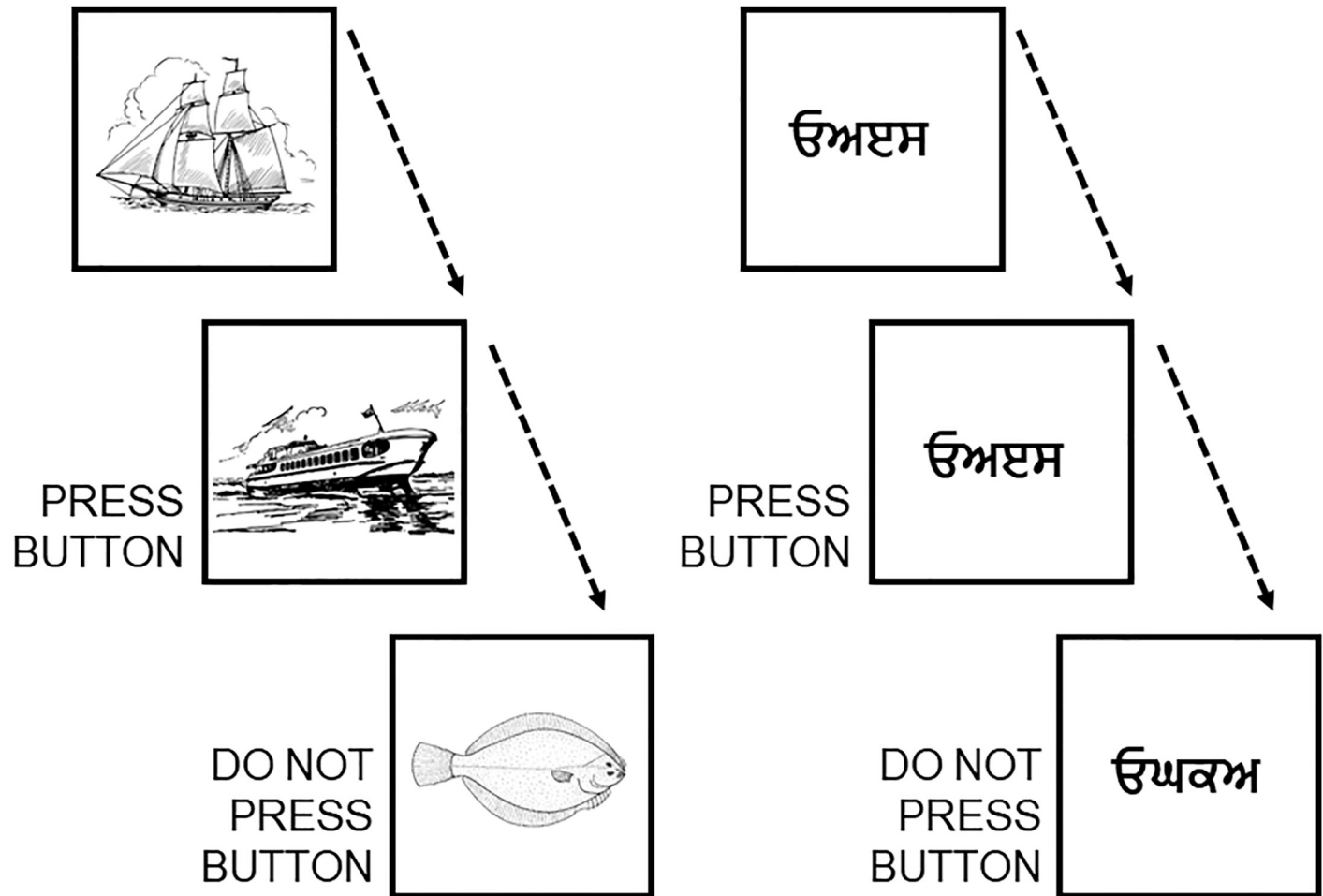
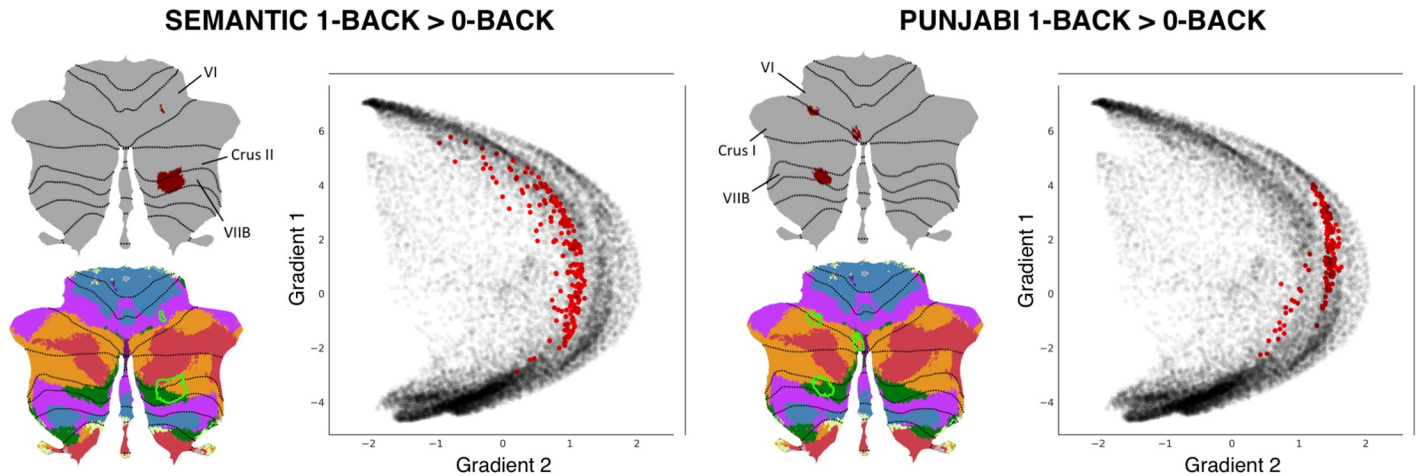


Fig 4. Scheme of the semantic 1-back condition and the visual (punjabi) 1-back condition.

<https://doi.org/10.1371/journal.pone.0210028.g004>

unfocused cognitive processing regions; perhaps contrasting with higher focused cognitive demands in the Punjabi task, which was located in aspects of task positive networks (dorsal/ventral attention, frontoparietal) that were slightly more distant from cerebellar default-mode network areas. LittleBrain offered an unparalleled visualization of this concept (Fig 5). The Punjabi task was located at high gradient 2 areas (corresponding to focused cognitive processing). The Semantic task was located at similar regions but extending towards higher gradient 1 values (i.e., more unfocused cognitive processing regions) and lower gradient 2 values (i.e., less focused cognitive processing regions). In this way, the Semantic task may engage cerebellar regions which are slightly less involved in focused cognitive processing when compared to the Punjabi task, and slightly more involved in unfocused cognitive processing. LittleBrain can thus capture subtle, progressive aspects of cerebellar functional neuroanatomy that would be difficult to visualize using conventional discrete parcellations of cerebellar functional neuroanatomy. Of note, comparison between gradients maps may be supplemented by additional statistical analyses—this possibility is explored in the following section.



**Fig 5. LittleBrain can capture subtle, progressive aspects of cerebellar functional neuroanatomy that would be difficult to visualize using conventional discrete parcellations of cerebellar functional neuroanatomy.** Both tasks engaged lobules VI, Crus I/II, and VIIIB. Both tasks engaged ventral/dorsal attention (green and purple) and frontoparietal (orange) networks (i.e., focused cognitive processing areas). Marginal aspects of default mode network (red) (i.e., unfocused cognitive processing areas) were included in the Semantic task only. The Semantic task may engage cerebellar regions which are slightly less involved in focused cognitive processing when compared to the Punjabi task, and slightly more involved in unfocused cognitive processing. LittleBrain provides an unparalleled visualization of this concept—the Semantic task reveals higher gradient 1 values (i.e., more unfocused cognitive processing regions) and lower gradient 2 values (i.e., less focused cognitive processing regions).

<https://doi.org/10.1371/journal.pone.0210028.g005>

### Flexibility examples

Our public source code repository (<https://github.com/xaviergp/littlebrain> [48]) includes several examples of alternative visualization and analysis strategies that users with coding experience might implement by interacting with the Jupyter notebook. These include (i) mapping multiple cerebellar clusters at once, each with a different color (Fig 6(A)), (ii) loading gradient 1 and 2 values for each voxel included within a cerebellar cluster and performing statistical analyses using these data (Fig 6(B)), and (iii) mapping cerebellar clusters using gradients other than 1 and 2 from Guell et al., 2018 [17] (e.g. using gradients 1 and 3) (Fig 6(C)). LittleBrain is therefore easy to install and use, but also allows the experienced user to develop complex novel visualization or analysis strategies. These alternative visualizations and analyses can be performed using Python packages included in our LittleBrain Docker container such as seaborn and scipy. Because LittleBrain is hosted publicly, users who develop new strategies may push their contributions back to the LittleBrain source code, or to the examples in the LittleBrain repository.

### LittleBrain manual

A manual with detailed download, installation, and use instructions is available at <https://xaviergp.github.io/littlebrain>.

### Discussion

We present LittleBrain, a novel neuroimaging data visualization tool that offers an unparalleled perspective to the topographical interpretation of cerebellar neuroimaging findings. Gradient-based approaches to brain function have recently unmasked fundamental properties of brain organization. LittleBrain applies this new knowledge to the topographical interpretation of cerebellar neuroimaging findings. It is an easily accessible, user-friendly tool that can also be interactively modified by experienced users.

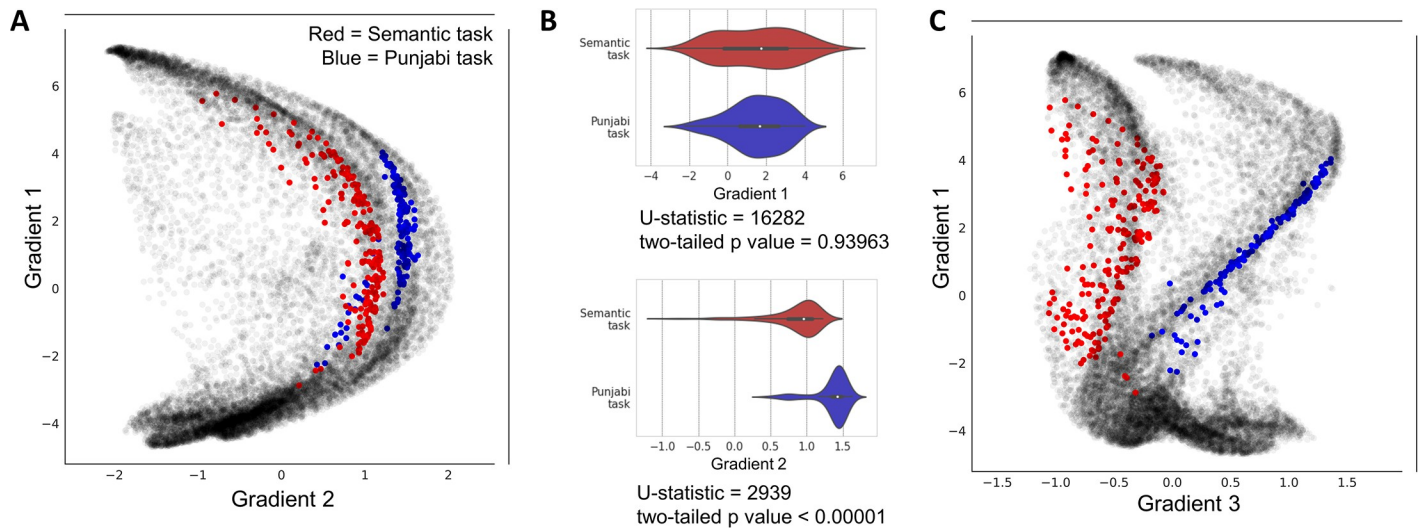


**Fig 6. Flexibility examples of LittleBrain using data from our previous example (Fig 5).** (A) Plotting two task maps in a single gradients map allows a better visualization of the relationship between them. Semantic task cluster is shown in red, Punjabi task cluster in shown in blue. (B) It is possible to load gradient 1 and gradient 2 values from each map (these values are automatically saved in the output folder), generate plots using these data (such as violin plots, as shown here), and also perform statistical tests using these data (such as Mann-Whitney tests, a non-parametric equivalent of a t-test, as shown here). This allowed us to detect, for instance, that gradient 2 but not gradient 1 differences between the two maps were statistically significant. (C) It is possible to use gradients other than gradients 1 or 2. For example, gradient 3 represents left-right hemisphere asymmetries in nonmotor cerebellar areas (see discussion in Guell et al., 2018 [17] regarding gradient 3). Accordingly, gradient 3 separates our two task maps given that they both engage non-motor processing areas, but are located at opposite cerebellar hemispheres (see Fig 5; Semantic task activation map is located in right cerebellar hemisphere while Punjabi task activation map is located in left cerebellar hemisphere).

<https://doi.org/10.1371/journal.pone.0210028.g006>

Using real data examples, we have shown that LittleBrain can provide alternative, gradual visualizations that complement traditional discrete parcellation maps of cerebellar functional neuroanatomy. We have also shown that LittleBrain can capture subtle, progressive aspects of cerebellar organization that would be difficult to visualize using conventional discrete parcellations. LittleBrain may thus improve the topographical interpretation of cerebellar neuroimaging findings, in a context where the cerebellum is receiving increased attention as a necessary component for understanding virtually all complex brain functions in health and disease.

Future research might expand the applications of the present work. For example, similar tools could be developed for the analysis of data from other brain regions. Margulies and colleagues [3] described functional gradients in the cerebral cortex—LittleBrain could be extended to operate on cerebral cortical data. Similarly, future tools may use gradient maps developed using methods other than resting-state diffusion map embedding, such as continuous semantic maps as developed by Huth and colleagues [7], continuous event timescale representation maps as developed by Baldassano and colleagues [8], or even continuous maps related to structural rather than functional brain properties [6].

Novel methods of analysis might also emerge from this new method of data visualization. As shown in Fig 6(B), statistical analyses might be performed using gradient values extracted from cerebellar clusters. Functional neuroanatomical differences between cerebellar clusters may therefore not only be visualized, but also quantified. Future research might explore the utility of this approach and determine the optimal strategy for such analyses.

Taken together, LittleBrain is a novel and fully functional tool that may significantly improve cerebellar neuroimaging data interpretation. It is accessible to the novice user, and transparent and flexible to the experienced user. It links novel developments in gradient-based functional neuroanatomy to the topographical interpretation of cerebellar neuroimaging findings, unmasking otherwise inaccessible functional properties of cerebellar data topography. It

resonates with a paradigm shift in the appreciation of the relevance of the cerebellum in neuroscience, and with an increased attention to gradient-based approaches to brain function in the neuroimaging community.

## Acknowledgments

The authors want to thank Paul Wighton for assistance when building Docker images, and Theodore LaGrow for participating in our toolbox name brainstorming.

## Author Contributions

**Conceptualization:** Xavier Guell.

**Formal analysis:** Xavier Guell.

**Investigation:** Xavier Guell.

**Methodology:** Xavier Guell.

**Software:** Xavier Guell, Mathias Goncalves, Jakub R. Kaczmarzyk.

**Supervision:** John D. E. Gabrieli, Jeremy D. Schmahmann, Satrajit S. Ghosh.

**Validation:** Xavier Guell.

**Visualization:** Xavier Guell.

**Writing – original draft:** Xavier Guell.

**Writing – review & editing:** John D. E. Gabrieli, Jeremy D. Schmahmann, Satrajit S. Ghosh.

## References

1. Gabrieli JDE, Ghosh SS, Whitfield-Gabrieli S. Prediction as a humanitarian and pragmatic contribution from human cognitive neuroscience. *Neuron*. 2015; 85(1):11–26. <https://doi.org/10.1016/j.neuron.2014.10.047> PMID: 25569345
2. Yeo B, Krienen FM, Sepulcre J, Sabuncu MR, Lashkari D, Hollinshead M, et al. The organization of the human cerebral cortex estimated by intrinsic functional connectivity. *J Neurophysiol*. 2011; 106(3):1125–65. <https://doi.org/10.1152/jn.00338.2011> PMID: 21653723
3. Margulies DS, Ghosh SS, Goulas A, Falkiewicz M, Huntenburg JM, Langs G, et al. Situating the default-mode network along a principal gradient of macroscale cortical organization. *Proc Natl Acad Sci*. 2016; 113(44):12574–9. <https://doi.org/10.1073/pnas.1608282113> PMID: 27791099
4. Coifman RR, Lafon S, Lee AB, Maggioni M, Nadler B, Warner F, et al. Geometric diffusions as a tool for harmonic analysis and structure definition of data: Multiscale methods. *Proc Natl Acad Sci*. 2005; 102(21):7432–7. <https://doi.org/10.1073/pnas.0500896102> PMID: 15899969
5. Huntenburg JM, Bazin PL, Margulies DS. Large-Scale Gradients in Human Cortical Organization. *Trends Cogn Sci*. 2018; 22(1):21–31. <https://doi.org/10.1016/j.tics.2017.11.002> PMID: 29203085
6. Huntenburg JM, Bazin PL, Goulas A, Tardif CL, Villringer A, Margulies DS. A Systematic Relationship Between Functional Connectivity and Intracortical Myelin in the Human Cerebral Cortex. *Cereb Cortex*. 2017; 27(2):981–97. <https://doi.org/10.1093/cercor/bhx030> PMID: 28184415
7. Huth AG, De Heer WA, Griffiths TL, Theunissen FE, Gallant JL. Natural speech reveals the semantic maps that tile human cerebral cortex. *Nature*. 2016; 532(7600):453–8. <https://doi.org/10.1038/nature17637> PMID: 27121839
8. Baldassano C, Chen J, Zadbood A, Pillow JW, Hasson U, Norman KA. Discovering Event Structure in Continuous Narrative Perception and Memory. *Neuron*. 2017; 95(3):709–721.e5. <https://doi.org/10.1016/j.neuron.2017.06.041> PMID: 28772125
9. Johansen-Berg H, Behrens TEJ, Robson MD, Drobniak I, Rushworth MFS, Brady JM, et al. Changes in connectivity profiles define functionally distinct regions in human medial frontal cortex. *Proc Natl Acad Sci*. 2004; 101(36):13335–40. <https://doi.org/10.1073/pnas.0403743101> PMID: 15340158
10. Jbabdi S, Sotiropoulos SN, Behrens TE. The topographic connectome. *Curr Opin Neurobiol*. 2013; 23(2):207–15. <https://doi.org/10.1016/j.conb.2012.12.004> PMID: 23298689

11. Haak K V., Marquand AF, Beckmann CF. Connectopic mapping with resting-state fMRI. *Neuroimage*. 2018; 170:83–94. <https://doi.org/10.1016/j.neuroimage.2017.06.075> PMID: 28666880
12. Schröder TN, Haak KV., Jimenez NIZ, Beckmann CF, Doeller CF. Functional topography of the human entorhinal cortex. *Elife*. 2015; 4:e06738.
13. Cerliani L, Thomas RM, Jbabdi S, Siero JCW, Nanetti L, Crippa A, et al. Probabilistic tractography recovers a rostrocaudal trajectory of connectivity variability in the human insular cortex. *Hum Brain Mapp*. 2012; 33(9):2005–34. <https://doi.org/10.1002/hbm.21338> PMID: 21761507
14. Bajada CJ, Jackson RL, Haroon HA, Azadbakht H, Parker GJM, Lambon Ralph MA, et al. A graded tractographic parcellation of the temporal lobe. *Neuroimage*. 2017; 155:503–12. <https://doi.org/10.1016/j.neuroimage.2017.04.016> PMID: 28411156
15. Jackson RL, Bajada CJ, Rice GE, Cloutman LL, Lambon Ralph MA. An emergent functional parcellation of the temporal cortex. *Neuroimage*. 2018; 170:385–99. <https://doi.org/10.1016/j.neuroimage.2017.04.024> PMID: 28419851
16. Marquand AF, Haak KV., Beckmann CF. Functional corticostriatal connection topographies predict goal-directed behaviour in humans. *Nat Hum Behav*. 2017; 1(8).
17. Guell X, Schmahmann J, Gabrieli J, Ghosh S. Functional gradients of the cerebellum. *Elife*. 2018; 7: e36652. <https://doi.org/10.7554/eLife.36652> PMID: 30106371
18. Schmahmann JD, Pandya DN. Projections to the basis pontis from the superior temporal sulcus and superior temporal region in the rhesus monkey. *J Comp Neurol*. 1991; 308(2):224–48. <https://doi.org/10.1002/cne.903080209> PMID: 1716269
19. Schmahmann JD. From movement to thought: Anatomic substrates of the cerebellar contribution to cognitive processing. *Hum Brain Mapp*. 1996; 4(3):174–98. [https://doi.org/10.1002/\(SICI\)1097-0193\(1996\)4:3<174::AID-HBM3>3.0.CO;2-0](https://doi.org/10.1002/(SICI)1097-0193(1996)4:3<174::AID-HBM3>3.0.CO;2-0) PMID: 20408197
20. Schmahmann JD, Pandya DN. Anatomic organization of the basilar pontine projections from prefrontal cortices in rhesus monkey. *J Neurosci*. 1997; 17(1):438–58. PMID: 8987769
21. Schmahmann JD, Pandya DN. The cerebrotocerebellar system. *Int Rev Neurobiol*. 1997; 41:31–60. PMID: 9378595
22. Middleton F a, Strick PL. Anatomical evidence for cerebellar and basal ganglia involvement in higher cognitive function. *Science (80-)*. 1994; 266(5184):458–61.
23. Schmahmann JD, Sherman JC. The cerebellar cognitive affective syndrome. *Brain*. 1998; 121(4):561–79.
24. Levisohn L, Cronin-Golomb A, Schmahmann JD. Neuropsychological consequences of cerebellar tumour resection in children. *Brain*. 2000; 123(5):1041–50.
25. Riva D. The cerebellum contributes to higher functions during development: Evidence from a series of children surgically treated for posterior fossa tumours. *Brain*. 2000; 123(5):1051–61.
26. Ravizza SM, McCormick CA, Schlerf JE, Justus T, Ivry RB, Fiez JA. Cerebellar damage produces selective deficits in verbal working memory. *Brain*. 2006; 129(2):306–20.
27. Schmahmann JD, Weilburg JB, Sherman JC. The neuropsychiatry of the cerebellum—Insights from the clinic. *Cerebellum*. 2007; 6(3):254–67. <https://doi.org/10.1080/14734220701490995> PMID: 17786822
28. Baillieux H, De Smet HJ, Paquier PF, De Deyn PP, Mariën P. Cerebellar neurocognition: Insights into the bottom of the brain. *Clin Neurol Neurosurg*. 2008; 110(8):763–73. <https://doi.org/10.1016/j.clineuro.2008.05.013> PMID: 18602745
29. Stoodley CJ, Schmahmann JD. Functional topography in the human cerebellum: A meta-analysis of neuroimaging studies. *Neuroimage*. 2009; 44(2):489–501. <https://doi.org/10.1016/j.neuroimage.2008.08.039> PMID: 18835452
30. Thompson RF, Steinmetz JE. The role of the cerebellum in classical conditioning of discrete behavioral responses. *Neuroscience*. 2009; 162(3):732–55. <https://doi.org/10.1016/j.neuroscience.2009.01.041> PMID: 19409234
31. Tedesco AM, Chiricozzi FR, Clausi S, Lupo M, Molinari M, Leggio MG. The cerebellar cognitive profile. *Brain*. 2011; 134(12):3669–83.
32. Stoodley CJ, Valera EM, Schmahmann JD. Functional topography of the cerebellum for motor and cognitive tasks: An fMRI study. *Neuroimage*. 2012; 59(2):1560–70. <https://doi.org/10.1016/j.neuroimage.2011.08.065> PMID: 21907811
33. Keren-Happuch E, Chen SHA, Ho MHR, Desmond JE. A meta-analysis of cerebellar contributions to higher cognition from PET and fMRI studies. *Hum Brain Mapp*. 2014; 35(2):593–615. <https://doi.org/10.1002/hbm.22194> PMID: 23125108

34. Koziol LF, Budding D, Andreasen N, D'Arrigo S, Bulgheroni S, Imamizu H, et al. Consensus paper: The cerebellum's role in movement and cognition. *Cerebellum*. 2014; 13(1):151–77. <https://doi.org/10.1007/s12311-013-0511-x> PMID: 23996631
35. Guell X, Hoche F, Schmahmann JD. Metalinguistic Deficits in Patients with Cerebellar Dysfunction: Empirical Support for the Dysmetria of Thought Theory. *Cerebellum*. 2015; 14(1):50–8. <https://doi.org/10.1007/s12311-014-0630-z> PMID: 25503825
36. Hoche F, Guell X, Sherman JC, Vangel MG, Schmahmann JD. Cerebellar Contribution to Social Cognition. *Cerebellum*. 2016; 15(6):732–43. <https://doi.org/10.1007/s12311-015-0746-9> PMID: 26585120
37. Hoche F, Guell X, Vangel M, Sherman J, Schmahmann J. The cerebellar cognitive affective/Schmahmann syndrome scale. *Brain*. 2018; 141(1):248–70. <https://doi.org/10.1093/brain/awx317> PMID: 29206893
38. Guell X, Gabrieli JDE, Schmahmann JD. Embodied cognition and the cerebellum: Perspectives from the Dysmetria of Thought and the Universal Cerebellar Transform theories. *Cortex*. 2018; 100:140–8. <https://doi.org/10.1016/j.cortex.2017.07.005> PMID: 28779872
39. Phillips JR, Hewedi DH, Eissa AM, Moustafa AA. The Cerebellum and Psychiatric Disorders. *Front Public Heal*. 2015; 3.
40. Wang T, Liu J, Zhang J, Zhan W, Li L, Wu M, et al. Altered resting-state functional activity in posttraumatic stress disorder: A quantitative meta-analysis. *Sci Rep*. 2016; 6.
41. Kim H, Kim J, Loggia ML, Cahalan C, Garcia RG, Vangel MG, et al. Fibromyalgia is characterized by altered frontal and cerebellar structural covariance brain networks. *NeuroImage Clin*. 2015; 7:667–77. <https://doi.org/10.1016/j.nicl.2015.02.022> PMID: 25844321
42. Guo CC, Tan R, Hodges JR, Hu X, Sami S, Hornberger M. Network-selective vulnerability of the human cerebellum to Alzheimer's disease and frontotemporal dementia. *Brain*. 2016; 139(5):1527–38.
43. Bastos Leite AJ, Van Der Flier WM, Van Straaten ECW, Scheltens P, Barkhof F. Infratentorial abnormalities in vascular dementia. *Stroke*. 2006; 37(1):105–10. <https://doi.org/10.1161/01.STR.0000196984.90718.8a> PMID: 16339463
44. Wolf RC, Thomann PA, Sambataro F, Wolf ND, Vasic N, Landwehrmeyer GB, et al. Abnormal cerebellar volume and corticocerebellar dysfunction in early manifest Huntington's disease. *J Neurol*. 2015; 262(4):859–69. <https://doi.org/10.1007/s00415-015-7642-6> PMID: 25626721
45. Wilkins A. Cerebellar dysfunction in multiple sclerosis. *Front Neurol*. 2017; 8.
46. Wu T, Hallett M. The cerebellum in Parkinson's disease. *Brain*. 2013; 136(3):696–709.
47. Arnold Anteraper S, Guell X, D'Mello A, Joshi N, Whitfield-Gabrieli S, Joshi G. Disrupted Cerebro-cerebellar Intrinsic Functional Connectivity in Young Adults with High-functioning Autism Spectrum Disorder: A Data-driven, Whole-brain, High Temporal Resolution fMRI Study. *Brain Connect*. 2018;
48. Guell X, Ghosh S. `xaviergp/littlebrain: Version v1_revision`. Zenodo. 2018;
49. Guell X, Gabrieli J DE, Schmahmann JD. Triple representation of language, working memory, social and emotion processing in the cerebellum: Convergent evidence from task and seed-based resting-state fMRI analyses in a single large cohort. *Neuroimage*. 2018; 172:437–49. <https://doi.org/10.1016/j.neuroimage.2018.01.082> PMID: 29408539
50. Buckner RL, Krienen FM, Castellanos A, Diaz JC, Yeo BTT. The organization of the human cerebellum estimated by intrinsic functional connectivity. *J Neurophysiol*. 2011; 106(5):2322–45. <https://doi.org/10.1152/jn.00339.2011> PMID: 21795627
51. Jenkinson M, Beckmann CF, Behrens TEJ, Woolrich MW, Smith SM. FSL. *Neuroimage*. 2012; 62(2):782–90. <https://doi.org/10.1016/j.neuroimage.2011.09.015> PMID: 21979382
52. Jenkinson M, Smith S. A global optimisation method for robust affine registration of brain images. *Med Image Anal*. 2001; 5(2):143–56. PMID: 11516708
53. Jenkinson M, Bannister P, Brady M, Smith S. Improved optimization for the robust and accurate linear registration and motion correction of brain images. *Neuroimage*. 2002; 17(2):825–41. PMID: 12377157
54. Fischl B. FreeSurfer. *Neuroimage*. 2012; 62(2):774–81. <https://doi.org/10.1016/j.neuroimage.2012.01.021> PMID: 22248573
55. Marcus DS, Harwell J, Olsen T, Hodge M, Glasser MF, Prior F, et al. Informatics and Data Mining Tools and Strategies for the Human Connectome Project. *Front Neuroinform*. 2011; 5.
56. Merkel D. Docker: lightweight Linux containers for consistent development and deployment. *Linux J*. 2014; 239(2).
57. Kaczmarzyk J, Goncalves M, Halchenko Y, Mitchell R, Nielson D, Jarecka D, et al. `kaczmarj/neurodocker: Version 0.4.0 release candidate 1 (Version 0.4.0rc1)`. Zenodo. 2018;
58. Chirigati F, Rampin R, Shasha D, Freire J. ReproZip: Computational Reproducibility With Ease. *Proc 2016 Int Conf Manag Data*. 2016;

59. Kluyver T, Ragan-kelley B, Pérez F, Granger B, Bussonnier M, Frederic J, et al. Jupyter Notebooks—a publishing format for reproducible computational workflows. *Positioning and Power in Academic Publishing: Players, Agents and Agendas*. 2016. 87–90 p.
60. Lesage E, Hansen PC, Miall RC. Right Lateral Cerebellum Represents Linguistic Predictability. *J Neurosci*. 2017; 37(26):6231–41. <https://doi.org/10.1523/JNEUROSCI.3203-16.2017> PMID: 28546307
61. Gorgolewski KJ, Varoquaux G, Rivera G, Schwartz Y, Sochat VV., Ghosh SS, et al. NeuroVault.org: A repository for sharing unthresholded statistical maps, parcellations, and atlases of the human brain. *Neuroimage*. 2016; 124:1242–4. <https://doi.org/10.1016/j.neuroimage.2015.04.016> PMID: 25869863
62. Stoodley CJ, Schmahmann JD. Evidence for topographic organization in the cerebellum of motor control versus cognitive and affective processing. *Cortex*. 2010; 46(7):831–44. <https://doi.org/10.1016/j.cortex.2009.11.008> PMID: 20152963